

GALACTIC DRIPS AND HOW TO STOP THEM

William G. Mathews

University of California Observatories/Lick Observatory
 Board of Studies in Astronomy and Astrophysics
 University of California, Santa Cruz, CA 95064
 mathews@ucolick.org

ABSTRACT

Under quite general conditions, the temperature of the hot interstellar gas at large radii in elliptical galaxies can be lower than the mean galactic virial temperature. If so, a nonlinear cooling wave can form in the hot interstellar gas and propagate slowly toward the galactic core at velocity $\sim 10 \text{ kpc Gyr}^{-1}$. If the cooling wave survives hydrodynamic instabilities, it can intermittently deposit cold gas within about ~ 15 effective radii. For a bright elliptical the total mass deposited in this manner is large, $\sim 0.3 \times 10^{10} M_{\odot}$. In contrast with *ad hoc* assumptions about “mass dropout” in galactic cooling flows, the galactic drip mechanism is a physically self consistent mechanism in which cold gas can derive from the hot interstellar gas far from the central regions of elliptical galaxies. If this cold gas forms into stars, it may account for the young stellar populations recently observed in many ellipticals. The existence of young stars and extended gas at $\sim 10^4 \text{ K}$ observed in some bright ellipticals may result from this galactic drip rather than galactic mergers. Galactic drips are expected in relatively isolated (field) ellipticals provided (i) the galactic stellar velocity ellipsoids are radially oriented at large galactic radii and (ii) the current Type Ia supernova rate is sufficiently small to be consistent with interstellar iron abundances found in recent X-ray studies.

Ellipticals located within clusters of galaxies are immersed in generally hotter cluster gas. If the pressure in the ambient cluster gas exceeds that in the outer parts of the galactic interstellar medium, some cluster gas can flow into the galaxy, increasing the gas temperature there and suppressing the appearance of galactic drips. Furthermore, the iron abundance in the galactic ISM can be *reduced* when an elliptical is surrounded by hot cluster gas.

Subject headings: galaxies: evolution, cooling flows, elliptical

1. INTRODUCTION

In this paper we describe a global thermal instability and nonlinear cooling wave that can develop naturally in the hot interstellar medium (ISM) of evolving elliptical galaxies. The ISM in elliptical galaxies arises from mass loss from an evolving population of old stars. Gas expelled from mass-losing stars into the ISM dissipates the kinetic energy inherited from the parent star and attains a temperature comparable to the galactic virial temperature ($T_{\text{vir}} \sim 10^{6.5} - 10^7 \text{ K}$). As a result the hot ISM occupies approximately the same volume as the visible stars. The hot ISM loses energy by radiative losses and slowly sinks in the galactic potential; this is a galactic cooling flow. Compression of the subsonically inflowing ISM by the galactic gravity field keeps the gas temperature nearly isothermal throughout most of the flow, but

radiative cooling losses ultimately dominate at the base of the flow where the plasma density is highest. The inflowing gas should cool toward a disk if the galaxy is rotating (Brighenti & Mathews 1996).

In this paper we describe the evolution of cooling flows in a typical large elliptical galaxy, demonstrating that a cooling wave – or galactic drip – instability can be expected quite generally provided (i) the Type Ia supernova rate is low (as recent X-ray observations suggest) and (ii) the stellar velocity ellipsoids are significantly radial at large galactic radii so that the effective stellar temperature in the outer galaxy is subvirial. This mass deposition from the ISM may have important implications for creating a subsystem of younger stars (Worthey et al. 1992; Worthey et al. 1995), in forming large, coherent filaments of cold gas far from the galactic cores (Trinchieri & di Serego Alighieri 1991) or possibly in creating regions of lower X-ray temperature (Kim & Fabbiano 1995). These galactic features have previously been identified with the residue of recent galactic mergers, but galactic drips may provide an alternative explanation. However, if the elliptical galaxy is located in a relatively dense cluster containing high-pressure cluster gas then the formation of galactic drips is suppressed.

2. DESCRIPTION OF THE GALACTIC MODEL

The evolution of galactic cooling flows is described by the usual equations of gas dynamics with additional source terms (Loewenstein & Mathews 1987; Brighenti & Mathews 1996). The continuity equation contains a source term $\alpha\rho_*(r)$ ($\text{gm s}^{-1} \text{cm}^{-3}$) representing the rate that new gas is introduced into the ISM by evolving stars of local space density ρ_* . Both mass-losing stars and supernovae are sources of gas, $\alpha = \alpha_* + \alpha_{sn}$, although $\alpha_* \gg \alpha_{sn}$. The momentum equation contains a gravitational term, including an important contribution from dark matter, and a sink term $-\alpha\rho_*u/\rho$, where u and ρ are the velocity and density of the local ISM. The sink term accounts for the momentum removed from the local flow in accelerating newly injected gas up to the local flow velocity.

The rate of change of the specific thermal energy ε is given by

$$\rho \frac{d\varepsilon}{dt} = \frac{P}{\rho} \frac{d\rho}{dt} - \frac{\rho^2 \Lambda(T)}{m_p^2} + \alpha_* \rho_* \left[\varepsilon_o - \varepsilon - \frac{P}{\rho} + \frac{u^2}{2} \right], \quad (2.1)$$

where $\Lambda(T)$ is the usual cooling coefficient for an optically thin plasma. The term $\varepsilon_o = 3kT_o/m_p$, where m_p is the proton mass, is the specific thermal energy corresponding to the mean injection temperature of stellar ejecta:

$$T_o = \frac{\alpha_*(t)T_*(r) + \alpha_{sn}(t)T_{sn}}{\alpha_* + \alpha_{sn}}. \quad (2.2)$$

In equation (2.1) $\varepsilon_o - \varepsilon$ represents the excess of total specific kinetic and thermal energy in stellar ejecta above that in the ambient plasma. A fraction $P/\rho\varepsilon$ of the energy of newly supplied gas is lost as the dense stellar ejecta does work against the ambient gas in achieving pressure balance. Finally a small amount of energy per gram $u^2/2$ is dissipated due to the motion of the cooling flow gas relative to the rest frame of the stars.

For simplicity and for comparison with other recent theoretical studies of galactic cooling flows we assume that the stellar mass is described with a simplified King model, $\rho(r) = \rho_{*o}[1 + (r/r_{*c})^2]^{-3/2}$ where r_{*c} is the stellar core radius. The mass distribution in the dark halo is described with a pseudo-isothermal profile, $\rho(r) = \rho_{ho}[1 + (r/r_{hc})^2]^{-1}$. Both density distributions terminate at some large radius $r = r_t$. The

galactic parameters that we adopt here are appropriate for a luminous elliptical lying on the fundamental plane (Dressler et al. 1987; Djorgovski & Davis 1987; Tsai & Mathews 1995; Brighenti & Mathews 1996). We assume that the total mass in the dark halo M_{ht} is nine times that in the stars M_{*t} . All relevant galactic parameters are listed in Table 1.

A self-consistent stellar temperature $T_*(r)$, required to determine the injection temperature $T_o(r)$, can be found by solving the equation of stellar hydrodynamics in the total galactic potential (Mathews 1988). Such a solution requires that some assumption be made about the variation of the stellar velocity ellipsoid with galactic radius. For this purpose we assume that the stellar orbits become progressively more radial as $r \rightarrow r_t$. Specifically, we adopt a velocity ellipsoid of the form

$$\frac{\langle v_r^2 \rangle - \langle v_{tr}^2 \rangle}{\langle v_r^2 \rangle} = \left(\frac{r}{r_t} \right)^q \quad (2.3)$$

where $\langle v_{tr}^2 \rangle$ and $\langle v_r^2 \rangle$ are the transverse and radial stellar velocity dispersions respectively. We choose $q = 2$, but the evolution of the ISM is not sensitive to the value of q over a wide range $1 \lesssim q \lesssim 3$. A preponderance of radial orbits is expected as a general result of many galactic formation models and is consistent with the anisotropic stellar pressure required to understand the observed flattening of massive ellipticals which is not due to galactic rotation. [We note however that oblate ellipticals can also be supported by increasing the azimuthal stellar velocity dispersion relative to the mean dispersion in the meridional plane (Satoh 1980).] However, a global instability in the stellar system toward growth of $l = 2$ modes is expected if the orbits are too radial (Polyachenko & Shukhman 1981). For stability it is necessary that $R_K \equiv 2K_r/K_t \lesssim 1.7 \pm 0.2$ where $K_r = \frac{1}{2} \int d^3v d^3x v_r^2 f$ and $K_t = \frac{1}{2} \int d^3v d^3x (v_\theta + v_\phi)^2 f$ are the kinetic energies in the radial and transverse directions (e.g. Bertin & Stiavelli 1993) and f is the stellar distribution function. For the orbital model described by equation (2.3) with $q = 2$ we find $R_K = 1.08$, which is safely stable. Finally, Tsai and Mathews (1995) have shown that mean stellar temperatures resulting from (2.3) are similar to those recently measured in the ISM of several bright ellipticals (Serlemitsos, et al. 1993; Mushotzky et al. 1994).

The rate coefficient for stellar mass loss $\alpha_*(t)$ for an old, single-burst stellar population can be represented quite accurately by a power law:

$$\alpha_s(t) = \alpha_*(t_{now})(t/t_{now})^{-p}$$

where $p = 1.3$ and $\alpha_*(t_{now}) = 5.4 \times 10^{-20} \text{ s}^{-1}$ is the current stellar mass loss rate (Mathews 1989) evaluated at $t_{now} = 15 \text{ Gyr}$. Fortunately p and $\alpha_*(t_{now})$ depend only very weakly on the poorly-known IMF (Mathews 1989).

Type Ia supernovae may supply additional energy to the cooling flow gas. The equivalent temperature of supernova ejecta in equation (2.2) is $T_{sn} = ME_{sn}/3km_{sn}$ where E_{sn} and m_{sn} are the energy and mass of material expelled in each supernova explosion. The Type Ia supernova rate observed in elliptical galaxies $\nu_{sn} = \alpha_{sn}M_{*t}/m_{sn}$ is usually characterized in SNu units, the number of supernovae in a 100 year interval from a stellar mass having luminosity $L_B = 10^{10}L_{B\odot}$. To represent α_{sn} in cgs units we use the mass to light ratio determined by van der Marel (1991): $M_{*t}/L_B = 2.98 \times 10^{-3}L_B^{0.35}h^{1.7}$ where $h = H/100$ is the reduced Hubble constant, taken as $h = 0.75$ here. Consolidating these results, the factor $\alpha_{sn}T_{sn}$ required for the injection temperature is

$$\alpha_{sn}T_{sn} = 2.13 \times 10^{-8} (E_{sn}/10^{51}\text{ergs}) h^{-1.7} L_B^{-0.35} \text{ SNu}(t) \text{ Ks}^{-1}. \quad (2.4)$$

The factor $\text{SNu}(t)$ describes the current and past supernova rate. The current value $\text{SNu}(t_{now})$, with $t_{now} = 15 \text{ Gyr}$, is poorly known from direct observation and its past behavior is very uncertain, evidently

depending on the exotic evolution of mass exchanging binary stars. Observed values of the supernova rate in elliptical galaxies, $\text{SNU}_{ob} \approx 0.2h^2$ (van den Bergh & McClure 1994; Cappellaro et al. 1993), are also poorly determined and differ in principle from SNU in equation (2.4) which is defined relative to other uncertain theoretical quantities (such as $E_{sn}/10^{51}$). Therefore $\text{SNU}(t_{now}) \sim \text{SNU}_{ob}$ is expected, but not exact equality. An upper limit on the value of $\text{SNU}(t)$ in equation (2.4) is provided by the iron abundance observed in the hot ISM; we assume that each Type Ia supernova releases $0.7 M_\odot$ of iron. Unfortunately this constraint on SNU is complicated by the uncertain amount of additional iron that accompanies normal stellar mass loss $\alpha_*\rho_*$ into the ISM. For the past history of Type Ia supernovae we adopt a simple power law with adjustable parameters:

$$\text{SNU}(t) = \text{SNU}(t_{now})(t/t_{now})^{-s} \quad (2.5)$$

with $s = 0.5$ or 1.0 (Loewenstein & Mathews 1991). Positive values of s correspond to the decline in supernova activity expected in cosmic evolution.

Additional iron is supplied to the ISM by normal stellar mass loss. For this purpose we adopt a stellar iron abundance given by

$$z_*(r) = 1.6z_\odot[1 + (r/r_{c*})]^{-m} \quad (2.6)$$

where $z_\odot = 1.77 \times 10^{-3}$ is the solar abundance. The iron abundance at the centers of bright ellipticals is generally thought to be in the range $1 - 2 z_\odot$. Regarding the exponent m , Thomsen & Baum (1989) find $z_*(R) \propto R^{-0.3}$ for the magnesium-index (Mg_2) gradient in terms of the projected radius R . Owing to the rapid decrease of stellar density with galactic radius, the variation of metallicity with physical radius, $z_*(r)$, is almost identical to that observed in projected light. But the iron abundance may not follow that of the magnesium index which itself is poorly known beyond an effective radius. In addition the iron abundances observed in the hot ISM are often much lower than those in stars within an effective radius. For these reasons we consider both $m = 0.3$ and $m = 1.3$ in equation (2.6).

The variation of the iron abundance in the ISM is described by

$$\frac{\partial \rho_z}{\partial t} + \frac{1}{r^2} \frac{\partial}{\partial r}(r^2 \rho_z u) = (\alpha_* z_* + \alpha_{sn} z_{sn}) \rho_*$$

where $z_{sn} \approx 0.5$ is the fraction of mass in Type Ia supernova that is iron and $\alpha_{sn} = 1.52 \times 10^{-17} h^{-1.71} L_B^{-0.354} \text{SNU}(t) \text{ s}^{-1}$. Throughout the following discussion of the evolution of the ISM and its iron abundance the only galactic parameters that are varied are m , $\text{SNU}(t_{now})$ and s .

3. THE GALACTIC DRIP PHENOMENON

The high iron abundance in the intercluster medium surrounding massive ellipticals, $z_{cl} \approx 0.3 - 0.4z_\odot$, indicates that strong galactic winds dominated the earliest galactic evolution. Since our interest here is specific to the later evolution of the ISM when cooling flows dominate, we begin the evolutionary calculation after the initial wind phase is assumed to have ended, at $t_1 = 1$ Gyr with a very low initial gas density, $\sim 10^{-4} \rho_*$. The spherically symmetric gas dynamical equations are integrated from t_1 to the present time, $t = t_{now} \equiv 15$ Gyr using a time dependent Lagrangian code. For the calculations described here the boundary condition at the outer boundary of the calculation $r = r_t$ is assumed to be a fixed wall, but calculations done with a free surface at $r = r_t$ give essentially the same results in all important respects. When gas cools to less than 3×10^4 K in a computational zone, it is removed from the calculation.

The temperature and number density profiles of three cooling flows are illustrated in Figure 1 at a variety of times for parameters $\text{SNU}(t_{\text{now}}) = 0.066, 0.022, 0.011$ all with $s = 1$, i.e. $\text{SNU}(t) \propto t^{-1}$. For the largest current supernova rate considered, $\text{SNU}(t_{\text{now}}) = 0.066$, the temperature and density evolve in a perfectly regular manner (panels a and b of Figure 1), just as expected for normal cooling flows. All the gas cools within the galactic core. However, when the current supernova rate is reduced to 0.022 (panels c and d), the gas temperature in the outer parts of the galaxy is smaller until age $t \sim 14$ Gyr and profile irregularities appear. With $\text{SNU}(t_{\text{now}}) = 0.011$ the irregularities in the flow propagate inward as seen in Figures 1e and 1f. In Figure 1e at $t = 6$ Gyrs a small temperature minimum appears at $\log r \approx 4.85$ which becomes more pronounced at times 8 and 10 Gyrs as it moves slowly toward the galactic center. The amplitude of the temperature minimum gradually increases as the cooling wave propagates inward, occasionally deepening catastrophically due to severe radiative losses. When the gas temperature drops below 3×10^4 K, the gas is removed from the hot phase of the ISM and begins to free fall in the galactic potential as it experiences a variety of hydrodynamic instabilities. This is the galactic drip.

Figure 2a illustrates the total mass of cold gas that drops out of these cooling flows beyond radius r for the $\text{SNU}(t_{\text{now}}) = 0.022$ and 0.011 solutions. In the latter case the mass drop-out beyond 5 kpc is large: $M_{\text{drop}}(r > 5) \approx 2 \times 10^9 M_{\odot}$. This is approximately equal to the total mass of hot gas remaining in the ISM after 15 Gyr, $M_{\text{gas}}(t_{\text{now}}) = 2.3 \times 10^9 M_{\odot}$. Also shown in Figure 2b is the times and galactic radii of the specific mass dropouts (where the temperature minimum drops below 3×10^4 K) as the galactic drip moves inward. For $\text{SNU}(t_{\text{now}}) = 0.011$ the drip starts at ≈ 72 kpc then slowly propagates toward the galactic core at velocity ~ 20 kpc Gyr $^{-1}$, reaching the center at $t = 10.5$ Gyr. None of these details of the cooling flow evolution depend on the assumed boundary condition at $r = r_t$ (fixed or free), on the size of the grid zoning, or on the criterion used to remove cold gas in the drips.

In addition to the deposition of cold gas by the cooling wave, Figure 2b also indicates that a significant mass of gas cools within about 5 kpc late in the cooling flow evolution for both values of $\text{SNU}(t_{\text{now}})$. This cooling occurs in numerous small drip events shown by the large number of points rising vertically at the left in Figure 2b. Although located at small galactic radii, this second type of cooling is well resolved by the numerical gas dynamics. This cooled gas may be optically visible since it is compressed by the high pressure ISM near the center of the galaxy.

When the past supernova rate is decreased by assuming $\text{SNU}(t) \propto t^{-0.5}$, or $s = 0.5$, galactic drips are more pronounced for fixed values of the current supernova rate $\text{SNU}(t_{\text{now}})$. Results for these calculations are shown in Figures 3 and 4. In contrast to the results in Figures 1a and 1b, Figures 3a and 3b and 4 show that an appreciable mass of cold gas drops out within about $r_e = 5$ kpc from the galactic center even for the largest current supernova rate $\text{SNU}(t_{\text{now}}) = 0.066$. This is evident in the intermittent irregularities visible in Figure 3a for times $t > 10$ Gyr. The total mass of cold gas that drips out is not small: $M_{\text{drop}}(r > 2\text{kpc}) \lesssim 0.4 \times 10^9 M_{\odot}$. As $\text{SNU}(t_{\text{now}})$ is decreased to 0.044 and 0.022, Figures 3c - 3f and 4 show that the cooling wave begins at earlier times in the calculation and at larger galactic radii. In Figure 3e the cooling wave moves to the origin before the time corresponding to the fourth temperature contour ($t = 10$ Gyr), but the inward motion of the cooling wave is nicely resolved in Figure 3c. In every case after a cooling wave reaches the center of the galaxy the temperature and density profiles return to their normal shapes.

3.1. Explanation of the Galactic Drip

Galactic drips arise when gas at great distances from the galactic center virializes locally to a temperature that is significantly less than that of the entire galaxy. This accumulation of cooler gas at large galactic radii is possible only if the supernova rate is sufficiently low. Most of the gas ejected from stars at large r is deposited early in the galactic evolution ($\alpha_* \propto t^{-1.3}$) when the assumed Type Ia supernova rate was also larger. At later times the supernova rate declines and the temperature of the cool, sub-virial gas drops further. Meanwhile the cool gas at large r goes into approximate freefall and accumulates where it encounters hot, pressure-supported gas at intermediate radii. The density at the base of the approximately freefalling gas becomes sufficiently large to initiate strong radiative cooling, a global thermal instability. As gravity pulls the relatively cool gas toward the galactic center, adjacent regions just beneath the cooling gas become compressed and the non-linear cooling wave slowly propagates inward in the galaxy, undergoing intermittent “mass dropouts” or “drips” when the radiative cooling time in the wave becomes very short. In the wake of the cooling wave, the ISM density, temperature and pressure are all lowered – in this sense the cooling wave resembles a phase change. Throughout the entire evolution the flow velocity is subsonic and the gas is in hydrostatic equilibrium to an excellent approximation.

Just before the cooling wave undergoes one of its episodic drips, there is a small density inversion in the wave. Such a condition will result in a localized Rayleigh-Taylor instability which is suppressed in the 1D calculation shown here. For this reason there is reason to believe that the evolution of the cooling wave after the first mass drop-out occurs may be geometrically more complicated than our 1D results suggest. If the wavefront becomes distorted, separate regions of cool gas may appear in the flow. It is possible, but far from proven, that this could account for the numerous cool inclusions which have been recently resolved by ROSAT PSPC observations in the outer parts of the cooling flow of the elliptical NGC 507 (Kim & Fabbiano 1995). Apart from this possible non-spherical distortion of the flow, our Lagrangian code is particularly well-suited to compute the evolution of the thermally cooling wave. The onset of catastrophic cooling in a small layer of gas can be masked by the zone-averaging procedures employed in Eulerian codes; this may explain why galactic drips have not been noticed in earlier theoretical calculations. Nevertheless, Fabrizio Brighenti (private communication) has successfully duplicated our results using 1D and 2D Eulerian codes, but only by using a very large number of computational zones.

The smooth, large scale subsonic velocity field in cooling flows (not shown in Figs. 1 and 2) becomes more irregular when the cooling drip occurs. Low-amplitude sound waves generated near the nonlinear cooling wave, particularly during mass dropout episodes, propagate outward in the galaxy retaining a modest amplitude as they move down the galactic density gradient.

3.2. ISM iron abundance and $\text{SNU}(t_{\text{now}})$

The iron abundance in the cooling flow gas depends on the stellar abundance variation with galactic radius and the current and past supernova rate. Recent determinations of the iron abundance in the hot ISM in elliptical galaxies are based on the equivalent width of the complex of FeL iron lines at ~ 1 keV. Abundances observed using the ASCA satellite are very low: Loewenstein et al. (1994) find $\langle z \rangle \approx 0.15$ in both NGC 1404 and NGC 4374; NGC 720, 1399, 4406, 4472 and 4636 have $\langle z \rangle \approx 0.3 - 0.4$ (Awaki, H. et al. 1994). Abundances based on the FeL feature should be accurate particularly for iron ions having only a few bound electrons that are most abundant at ISM temperatures $T \gtrsim 10^7$ K. Therefore the FeL abundances should be reliable for most massive ellipticals. The mean *stellar* abundance based on equation (2.6) is $\langle z_* \rangle = 0.63z_\odot$ if $m = 0.3$ and $\langle z_* \rangle = 0.11z_\odot$ if $m = 1.3$. These mean stellar abundances provide

definite lower limits on the iron abundance in the ISM since the additional iron contributed by supernovae can only raise it further. Obviously, no ISM model computed with $z(0) = 1.6z_\odot$ and $m = 0.3$ can match the ISM iron abundances measured in NGC 1404 and NGC 4374. Models assuming $m = 1.3$ (for which there is no observational support) do have lower mean iron abundances, but still exceed those observed.

Table 2 lists mean iron abundances in the ISM $\langle z(r)/z_\odot \rangle$ for nine cooling flow models at time $t = 15$ Gyr. Very few of these values are as low as those observed in the ISM by the ASCA satellite. The apparent discrepancy between the stellar iron abundances, the observed Type Ia supernova rate and the ASCA iron abundances in the hot gas is an outstanding problem that is currently unresolved. Nevertheless, the parameters s and $\text{SNu}(t_{\text{now}})$ used here to describe the past and present Type Ia supernova rate in the cooling flow models shown in Figures 1 - 4 are not too small; the discrepancy between the iron abundances found in the models shown in Table 2 and the ASCA values would only be larger if s and $\text{SNu}(t_{\text{now}})$ were increased sufficiently to inhibit galactic drips. We conclude that galactic drips should be a common occurrence in elliptical galaxies.

3.3. What Happens to the Gas that Cools?

The final state of the cooled off gas is uncertain, particularly since magnetic stresses are likely to play a significant role as the density increases in the dripping gas. If we assume nevertheless that the cold gas is able to form into stars, the total mass of young stars is small compared to the older stellar population, $M_{dt}(r > 0.5\text{kpc}) \lesssim 5 \times 10^{-3} M_{*t}$. The luminosity of a hypothetical population of young stars formed from this gas can be estimated by assuming that they form immediately after mass dropout and decline in luminosity according to the single burst luminosity evolution (with Salpeter IMF) described by Bruzual and Charlot (1993). For most of the ISM calculations with mass dropout shown in Figures 2 and 4 the resulting approximate luminosity of young stars is $L_{Bd}(t_{\text{now}}) \approx 2 - 6 \times 10^8 L_{B\odot}$. This is a small fraction of the total B-band luminosity of the galaxy, $L_B = 4.95 \times 10^{10} L_{B\odot}$. In two cases, however, the last mass dropout before the calculation was terminated at $t_{\text{now}} = 15$ Gyr is so recent that the luminosity of young stars is rather large: $L_{Bd}(t_{\text{now}}) \approx 9 \times 10^9 L_{B\odot}$ ($s = 1$; $\text{SNu}(t_{\text{now}}) = 0.022$) and $L_{Bd}(t_{\text{now}}) \approx 5 \times 10^9 L_{B\odot}$ ($s = 0.5$; $\text{SNu}(t_{\text{now}}) = 0.044$). Of course these estimates in which stars are assumed to form with a normal IMF in this unusual environment are very uncertain. It is possible nevertheless that young stars formed in drips could contribute in an important way to the photometric $H\beta$ index (a signature of youthful stars) observed in many ellipticals by Worthey, Faber and Gonzalez (1992).

The total mass of gas deposited by cooling waves beyond several kpc, $M_{dt} \lesssim 3 \times 10^9 M_\odot$, although small compared to the mass of old stars, is often comparable with the total mass of hot gas remaining in the cooling flow after $t_{\text{now}} = 15$ Gyr, $M_g(t_{\text{now}}) \sim 2 - 6 \times 10^9 M_\odot$. If some of this cooled-off gas resides for a time in pressure equilibrium with the local hot gas and is kept ionized by galactic UV radiation (Mathews 1990), it could account for the large scale, asymmetric $H\alpha$ filaments extending out to at least ~ 10 kpc observed in many bright ellipticals (Trinchieri & di Serego Alighieri 1991). The cooling gas in the outer parts of galactic cooling flows may also be related to the numerous islands of cool gas recently resolved by the ROSAT satellite in the X-ray image of NGC 507 (Kim & Fabbiano 1995).

4. ELIMINATION OF DRIPS BY CLUSTER GAS

For galactic drips to occur it is necessary that the supernova rates and stellar temperatures be rather low at large galactic radii, although both conditions seem easy to justify. The influence of various supernova rates on drip formation is illustrated in Figures 1 - 4. To gain insight into the influence of stellar temperature on galactic drips, several calculations were repeated with different values of q in equation (2.3). We find that the cooling flow patterns are not critically sensitive to this parameter. In another experiment the galactic stars were divided into two distributions, one having velocity ellipsoids as described by equation (2.3) and a second having purely circular orbits (which have the largest possible temperature T_* at a given r). Typically we find that galactic drips appear in the flow unless more than half of the stars beyond $\sim 10r_e$ have highly tangential (i.e. circular) orbits. Since geometric flattening in ellipticals depends on a strong radial component in the stellar orbits, we conclude that equation (2.3) is a reasonable model.

In addition to adjusting internal parameters, it is also possible to suppress drips by immersing a drip-prone galaxy in hot cluster gas. Even when the velocity of the elliptical is small relative to the ambient gas, some hot cluster gas can move into the galaxy, physically displacing the outer ISM and heating it by compression.

To illustrate this latter effect, the evolutionary ISM calculation for the elliptical having parameters $s = 0.5$, $\text{SNU}(t_{\text{now}}) = 0.022$ and $m = 1.3$, which generated drips in Figures 3e, 3f and 4b, was repeated in a relatively high pressure cluster environment. At present we have only a poor understanding of the evolution of cluster gas, but it is likely that gas observed in clusters today has evolved significantly during the last few Gyr and may still be highly transient in many clusters. In order to illustrate the influence of ambient cluster gas on the galactic drip phenomenon, we assume for simplicity that the cluster gas has been in existence with its present-day properties since $t_1 = 1$ Gyr and that there is no appreciable motion of the galaxy relative to the cluster gas. At t_1 the cluster gas is assumed to be isothermal at $T_{cl} = 10^8$ K and in hydrostatic equilibrium in the galactic potential before the evolution of the galactic ISM is begun. As the galactic ISM evolves, its cooling flow is born into the preexisting cluster environment. The cluster gas is assumed to extend to a fixed wall at 1 Mpc where its (initial) density is $n_{cl} = 10^{-4} \text{ cm}^{-3}$. The initial cluster gas density, in isothermal hydrostatic equilibrium in the galactic potential, increases to $n_{cl} = 2.5 \times 10^{-4} \text{ cm}^{-3}$ at the galactic center. These cluster gas parameters have been chosen so that the radiative cooling time beyond the physical limit of the galaxy ($r > r_t$) exceeds 15 Gyr. During the ensuing evolution the ambient density and temperature in the cluster gas ($r_t \leq r \leq 1 \text{ Mpc}$) remain approximately constant although some of the cluster gas initially beyond r_t flows into the galaxy. Since the pressure of the ambient hot cluster gas does not vary appreciably, the evolution of the galactic ISM is astronomically unrealistic, but we can suppose that the final state after $t = 15$ Gyr provides a reliable indication of the present-day influence of the cluster environment on the ISM.

Figure 5 compares the galactic cooling flow after $t = 15$ Gyr for the isolated galaxy with an identical galaxy that has evolved in the cluster environment as described above. The increased gas temperature and density and altered iron abundance within the galactic boundary (at $\log r_t = 5.05$) relative to the isolated galaxy (long-short dashed lines) all arise due to the flow of cluster gas into the galaxy. In particular the temperature profile in the cluster galaxy (solid line in Figure 5a) increases with radius beyond r_e , ultimately joining the temperature 10^8 K of the ambient cluster gas. The gas temperature in the outer parts of the galaxy is increased due to thermal mixing with the hot cluster gas that flows into the galaxy and from the compression of galactic gas by the ambient pressure which exceeds that in the galactic ISM at $r \sim r_t$. Since the gas temperature is kept high everywhere in the flow, no galactic drips occurred in the cluster galaxy during its entire evolution leading up to the final configuration shown in Figure 5.

When the galaxy is immersed in cluster gas, the gas density variation in the outer galaxy is less steep

(solid line in Figure 5b). This will result in a shallower X-ray surface brightness profile than that of the isolated (field) galaxy.

In view of the low iron abundances in the hot gas determined by ASCA, some authors have questioned whether the metallicity of the cluster gas can influence that of the galaxy. For insight into this question, we illustrate in Figure 5c the iron abundance at $t = 15$ Gyr in the galactic ISM for a galaxy having a stellar metallicity characterized by a power law index $m = 1.3$ in equation (2.6). The cluster gas is assumed to have abundance $z/z_{\odot} = 0.4$. It is clear from Figure 5c that the overall ISM metallicity of cluster galaxies *can* be influenced by the flow of cluster gas into the galaxy. The iron abundance $z(r)/z_{\odot}$ for the isolated galaxy (long-short dashed line) is actually *higher* than that for the same galaxy when placed in the iron-rich cluster environment (solid line)! The explanation of the sense of this difference is that the inward flow velocity is increased somewhat when the galaxy is surrounded by high pressure cluster gas. The iron abundance in the faster moving cooling flow gas is lower since it experiences fewer supernova events during its shorter flow time to the galactic center. Paradoxically, therefore the iron abundance in an elliptical ISM can be *reduced* by placing it in a hot cluster of even higher iron abundance!

5. DISCUSSION AND SUMMARY

Galactic drips can occur in isolated ellipticals whenever (i) the Type Ia supernova rate is low enough to be (more) consistent with observed iron abundances in the ISM and (ii) provided the stellar orbits become preferentially radial in the outer galaxy, leading to relatively low stellar temperatures $T_*(r)$. This latter condition is consistent with the asymmetric stellar pressure required to flatten ellipticals having very low rotation velocities. When these conditions are satisfied, a global thermal instability can form in the ISM, initiating a cooling wave that propagates slowly inward. Should finite aspherical density or temperature perturbations with appreciable amplitudes exist in the wave region, the subsequent evolution of the wave may be geometrically complex, but it is not clear why such perturbations would be expected. If the cooling wave develops in a quiescent galactic atmosphere, as we assume here, it slowly propagates toward the galactic center, experiencing episodes of precipitous cooling (drips) which can deposit substantial masses ($\sim 0.2 - 0.3 \times 10^{10} M_{\odot}$) of cold ($T \lesssim 10^4 \text{K}$) gas within about $15 r_e$. In addition to this sequence of drips, a significant amount of gas can cool within the brightest parts of the elliptical, $r \lesssim r_e$, in a multitude of drips confined to this region. If the cooled-off gas eventually forms into stars, as many authors have assumed, it may be sufficient to account for the populations of young stars reported by Worthey, Faber, & Gonzalez (1992). Unfortunately, the physics of such a star formation process remains obscure.

In many theoretical models of spherical galactic cooling flows it has been assumed that cold gas can condense directly from the hot ISM in thermally unstable regions located far from the galactic center (Stewart et al. 1984; Thomas et al. 1987; White & Sarazin 1987a, 1987b, 1988; Bertin & Toniazzo 1995). This assumption was found to be useful to reduce the theoretical X-ray surface brightness near the galactic cores to agree with surface brightness distributions observed in three bright Virgo ellipticals (Canizares, Fabbiano, & Trinchieri 1987). Unfortunately it has subsequently been shown that low amplitude perturbations are not generally thermally unstable (Balbus 1991) while finite amplitude perturbations disrupt rapidly as a result of shear and Rayleigh-Taylor instabilities (Hattori & Habe 1990; Malagoli et al. 1990). In addition, there is no natural way for finite perturbations to arise in the ISM (Mathews 1990). It is more likely that the effects of galactic rotation (Brighenti & Mathews 1996) and magnetic field, which are not included in the studies above, must be considered in comparing theoretical and observed surface

brightness distributions near galactic cores. However, the galactic drip phenomenon described here does provide a physically plausible mechanism for thermal instabilities to develop directly from the hot gas at large galactic radii. Nevertheless drips cannot provide a general explanation for the relatively flat central X-ray surface brightness distributions for ellipticals since the cooling wave that produces the drip is a transient effect that cannot be synchronized in all galaxies. Moreover, it seems likely that the environmental influences of companion galaxies and randomly infalling gas in the (poorly understood) outermost parts of real ellipticals could introduce a non-spherical character to the initial growth of galactic drips. In addition, perfectly spherical ellipticals are rare in nature. Therefore in the absence of multidimensional theoretical studies, it can be doubted that cooling flows in real ellipticals evolve in the idealized spherical manner shown in Figures 1-4 all the way to the galactic centers. Since it is likely that cooling waves may not be spatially coherent on spherical surfaces, the evolution of the soft X-ray luminosity and surface brightness profiles corresponding to Figures 1-4 has not been emphasized here.

Galactic drips can be suppressed in three ways: (i) by increasing the current or past theoretical supernova rate, (ii) by assuming that a large fraction (at least half) of the galactic stars have tangential orbits at large radii ($r \gtrsim 10r_e$), or (iii) by immersing the galaxy in hot cluster gas. The first means of avoiding drips is unacceptable since the global iron abundance would be too high at the current time, even if the stellar iron abundance drops much faster with galactic radius than is commonly thought. The second means of suppressing drips, by introducing tangential stellar orbits at great distances, may be inconsistent with models of elliptical formation that have a significant dissipationless character. But in any case, strongly radial orbits are required to account for the anisotropic stellar pressure support that prevails in luminous, non-spherical ellipticals. Therefore the primary mechanism to avoid galactic drips may be cluster membership. If star formation results from galactic drips, field ellipticals should exhibit more evidence of recent star formation (larger $H\beta$ indices) than cluster members. It is therefore quite remarkable that precisely this result has been reported by Worthey, Trager, & Faber (1995). These authors find that the incidence of a population of younger stars is almost (perhaps totally) a property of field ellipticals while cluster ellipticals seem to have little or no evidence of youthful stars.

This last result may be understood alternatively as a consequence of galactic mergers which are expected to be more common for field galaxies. Although very clear evidence for recent mergers exists in some ellipticals, it is far from proven that mergers are the dominant ongoing evolutionary process in these galaxies at the present time or in the recent past. We have shown here that the appearance of young stars, transient filaments of ionized gas and cool X-ray inclusions are not unambiguous signatures of recent mergers, but may instead result from galactic drips, a natural development in the evolution of galactic cooling flows. Finally, we note that the iron abundance in galactic cooling flows can be *lowered* when the galaxy is located in high pressure, iron-rich cluster gas; this may account in part for some of the remarkably low iron abundances that have been observed in the hot ISM of some ellipticals.

WGM thankfully acknowledges support from CalSpace, a Faculty Research Grant from UCSC and NASA grant NAG 5-3060. Thoughtful remarks and advice from Fabrizio Brighenti, Sandra Faber, Mike Loewenstein, Scott Trager, and John Tsai are acknowledged with thanks.

REFERENCES

- Awaki, H. et al. 1994, PASJ, 46, L65
- Balbus, S. A. 1991, ApJ, 372, 25
- Bertin, G., & Stiavelli, M. 1993, Rep. Prog. Phys., 56, 493
- Bertin, G., & Toniazzi, T. 1995, ApJ, 451, 111
- Brighenti, F. & Mathews, W. G. 1996, ApJ (in press)

- Bruzual, A. G., & Charlot, S. 1993, *ApJ*, 405, 538
- Canizares, C. R., Fabbiano, G. & Trichieri, G. 1987, *ApJ*, 312, 503
- Cappellaro, E. et al. 1993, *A&A*, 273, 383
- Djorgovski, S., & Davis, M., 1987, *ApJ*, 313, 59
- Donnelly, R. H., Faber, S. M., & O’Connell, R. M. 1990, *ApJ*, 354, 52
- Dressler, A., Lynden-Bell, D., Burstein, D., Davies, R.L., Faber, S. M., Terlevich, R. J., & Wegner, G. 1987, *ApJ*, 313, 42
- Hattori, M. & Habe, A. 1990, *MNRAS*, 242, 399
- Kim, Dong-Woo, & Fabbiano, G. 1995, *ApJ*, 441, 182
- Loewenstein, M., & Mathews, W. G. 1987, *ApJ*, 319, 614
- Loewenstein, M. & Mathews, W. G., 1991, *ApJ*, 373, 445
- Loewenstein, M., Mushotzky, R. F., Tamura, T., Ikebe, Y., et al. 1994, *ApJ*, 436, L75
- Malagoli, A., Rosner, R. & Fryxell, B. 1990, *MNRAS*, 247, 367
- Mathews, W. G. 1988, *AJ*, 95, 1047
- Mathews, W. G. 1989, *AJ*, 97, 42
- Mathews, W. G. 1990, *ApJ*, 354, 468
- Mushotzky, R. F., Loewenstein, M., Awaki, H., Makishima, K., Polyachenko, V. L., & Shukhman, I G. 1981, *Sov. Astron.-AJ*, 25, 533
- Satoh, C. 1980, *PASJ*, 32, 41
- Serlemitsos, P. J., Loewenstein, M., Mushotzky, R. F., Marshall, F. E. 1993, *ApJ*, 413, 518
- Stewart, G. C., Canizares, C. R., Fabian, A. C., & Nulsen, P. E. J. 1984, *ApJ*, 278, 536
- Thomas, P. A., Fabian, A. C., & Nulsen, P. E. J. 1987, *NMRAS*, 228, 973
- Thomsen, B., & Baum, W. A. 1989, *ApJ*, 347, 214
- Trinchieri, G., & di Serego Alighieri, S. 1991, *AJ*, 101, 1647
- Tsai, J. C., & Mathews, W. G. 1995, *ApJ*, 448, 84
- van den Bergh, S. & McClure, R. D. 1994, *ApJ*, 425, 205
- van der Marel, R. P., 1991, *MNRAS*, 253, 710
- White, R. E. & Sarazin, C. L. 1987a, *ApJ*, 318, 612
- White, R. E. & Sarazin, C. L. 1987b, *ApJ*, 318, 621
- White, R. E. & Sarazin, C. L. 1988, *ApJ*, 335, 688
- Worthey, G., Faber, S. M., & Gonzalez J. J., 1992, *ApJ*, 398, 69
- Worthey, G., Trager, S. C., & Faber S. M. 1995 (in preparation)

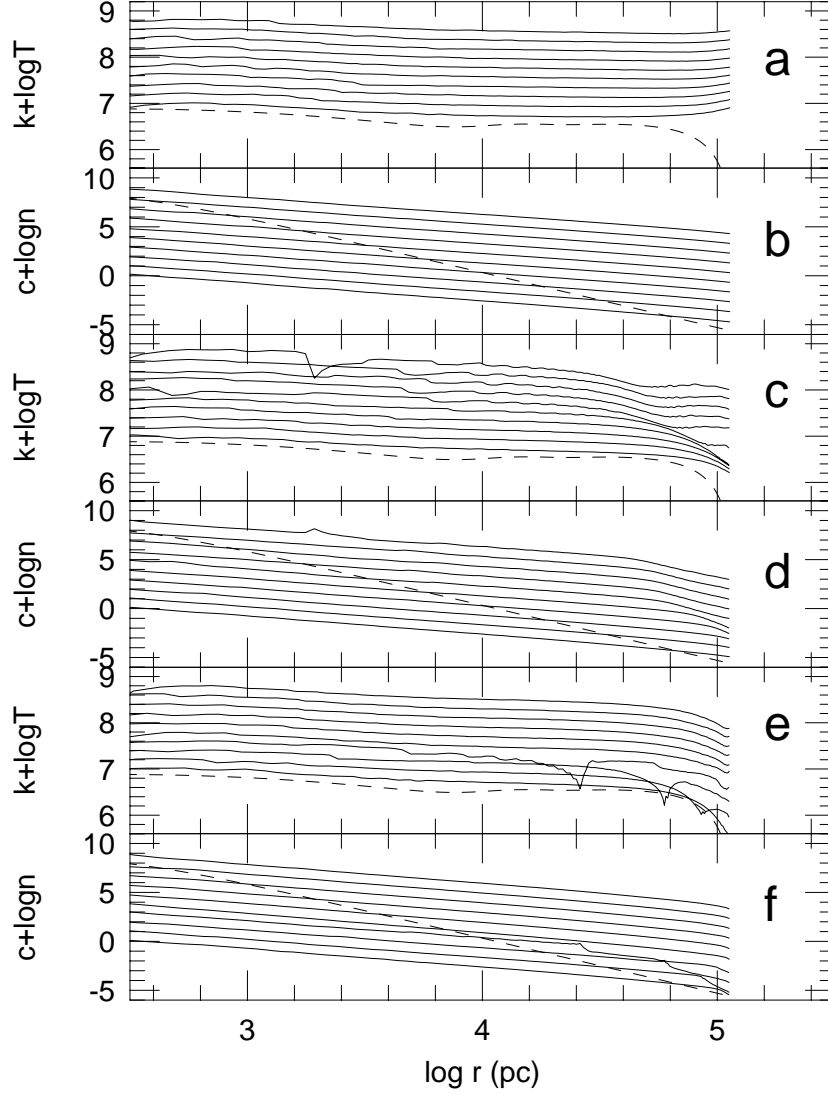


Fig. 1.— Temperature and number density evolution in the ISM of a massive elliptical when $s = 1$ shown for three values of $\text{SNU}(t_{\text{now}})$. Profiles of $T(r, t)$ and $n(r, t)$ are shown at ten times: 4, 6, 8, 10, 12, 13.91, 14.31, 14.51, 14.61, and 15.0 Gyrs. For clarity the profiles have been shifted vertically; the constants on the vertical axes are $k = 0.2(n - 1)$ and $c = 0.1(n - 1)$ where $n = 1 - 10$ corresponds to each of the ten times above. The stellar temperature $T_*(r)$ (normalized with $k = 0$) and density $\rho_*(r)$ (unnormalized) are shown with dashed lines. (*a and b*): Temperature and density variation with $\text{SNU}(t_{\text{now}}) = 0.066$; (*c and d*): Temperature and density variation with $\text{SNU}(t_{\text{now}}) = 0.022$; (*e and f*): Temperature and density variation with $\text{SNU}(t_{\text{now}}) = 0.011$.

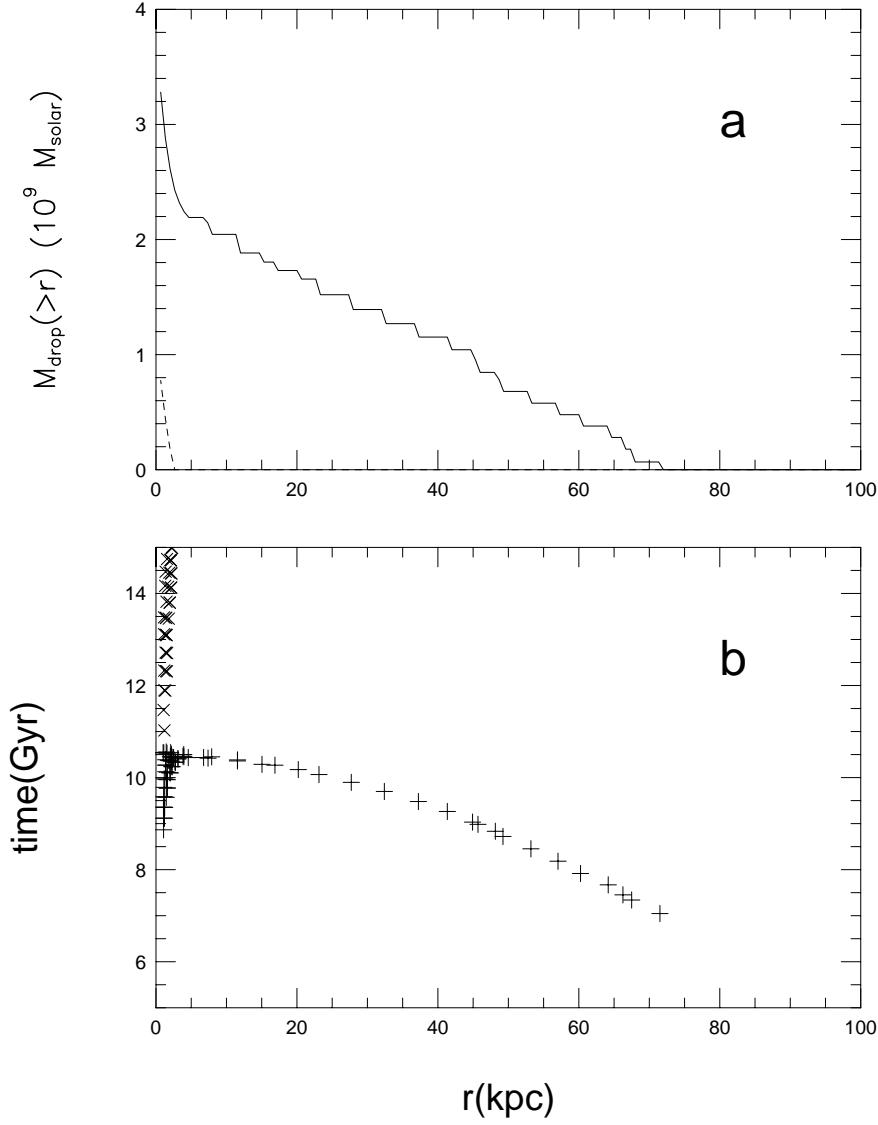


Fig. 2.— ISM evolution with $s = 1$. (a) Total mass of gas dropped out beyond radius r , $M_{\text{drop}}(>r)$ when $\text{SNU}(t_{\text{now}}) = 0.022$ (dashed line) and $\text{SNU}(t_{\text{now}}) = 0.011$ (solid line). (b) Radii and times of individual drip events in $r > 0.5$ kpc when $\text{SNU}(t_{\text{now}}) = 0.022$ (crosses) and $\text{SNU}(t_{\text{now}}) = 0.011$ (plus signs).

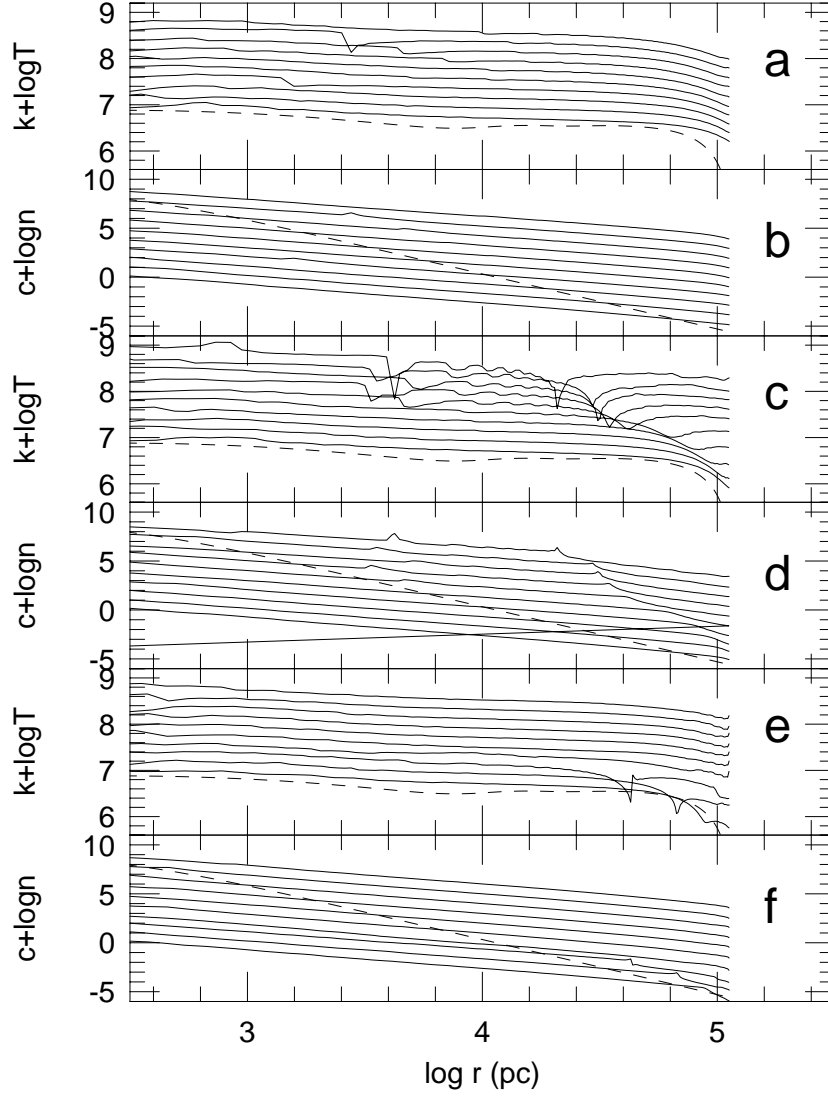


Fig. 3.— Temperature and number density evolution in the ISM of a massive elliptical when $s = 0.5$. All times and stellar profiles are identical to those in Figure 1. (*a and b*): Temperature and density variation with $\text{SNU}(t_{\text{now}}) = 0.066$; (*c and d*): Temperature and density variation with $\text{SNU}(t_{\text{now}}) = 0.044$; (*e and f*): Temperature and density variation with $\text{SNU}(t_{\text{now}}) = 0.022$.

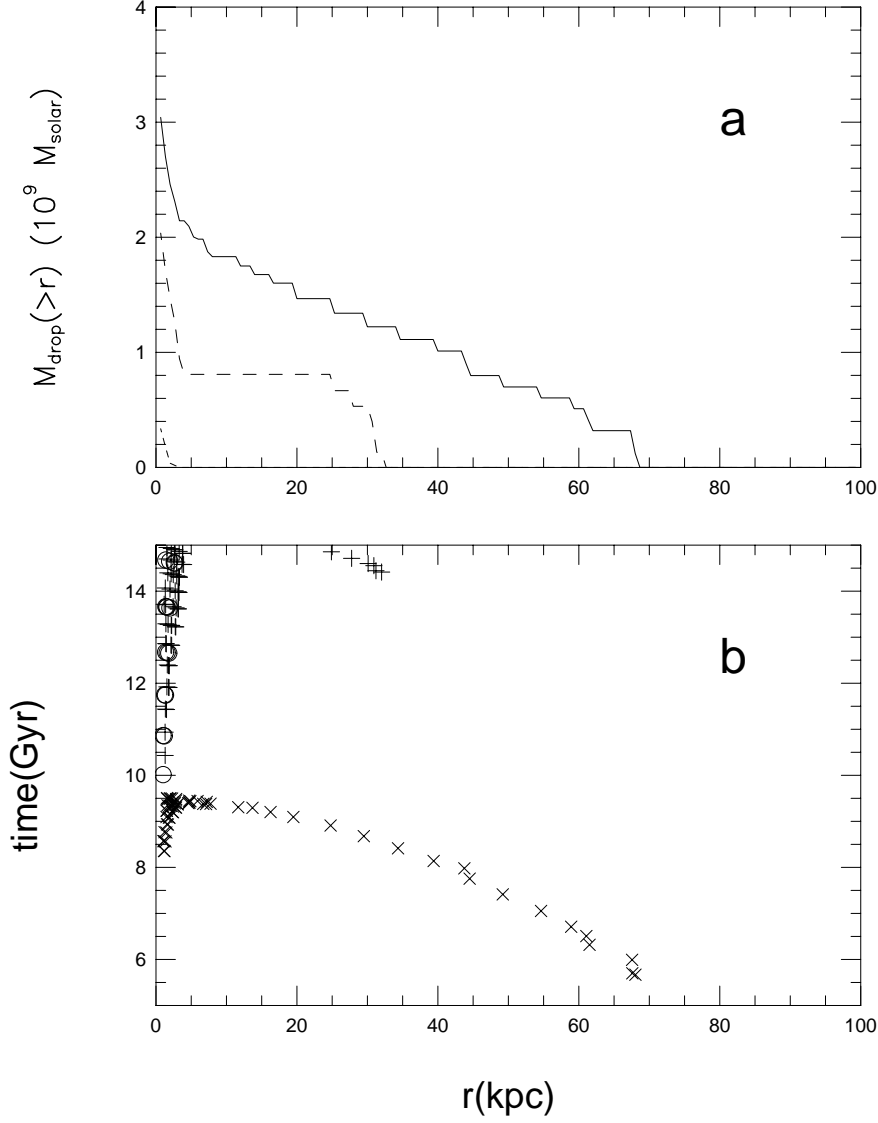


Fig. 4.— ISM evolution with $s = 0.5$. (a) Total mass of gas dropped out beyond radius r , $M_{\text{drop}}(> r)$ when $\text{SNU}(t_{\text{now}}) = 0.066$ (short dashed line) $\text{SNU}(t_{\text{now}}) = 0.044$ (long dashed line) and $\text{SNU}(t_{\text{now}}) = 0.022$ (solid line). (b) Radii and times of individual drip events in $r > 0.5$ kpc when $\text{SNU}(t_{\text{now}}) = 0.022$ (crosses), $\text{SNU}(t_{\text{now}}) = 0.044$ (plus signs) and $\text{SNU}(t_{\text{now}}) = 0.066$ (open circles).

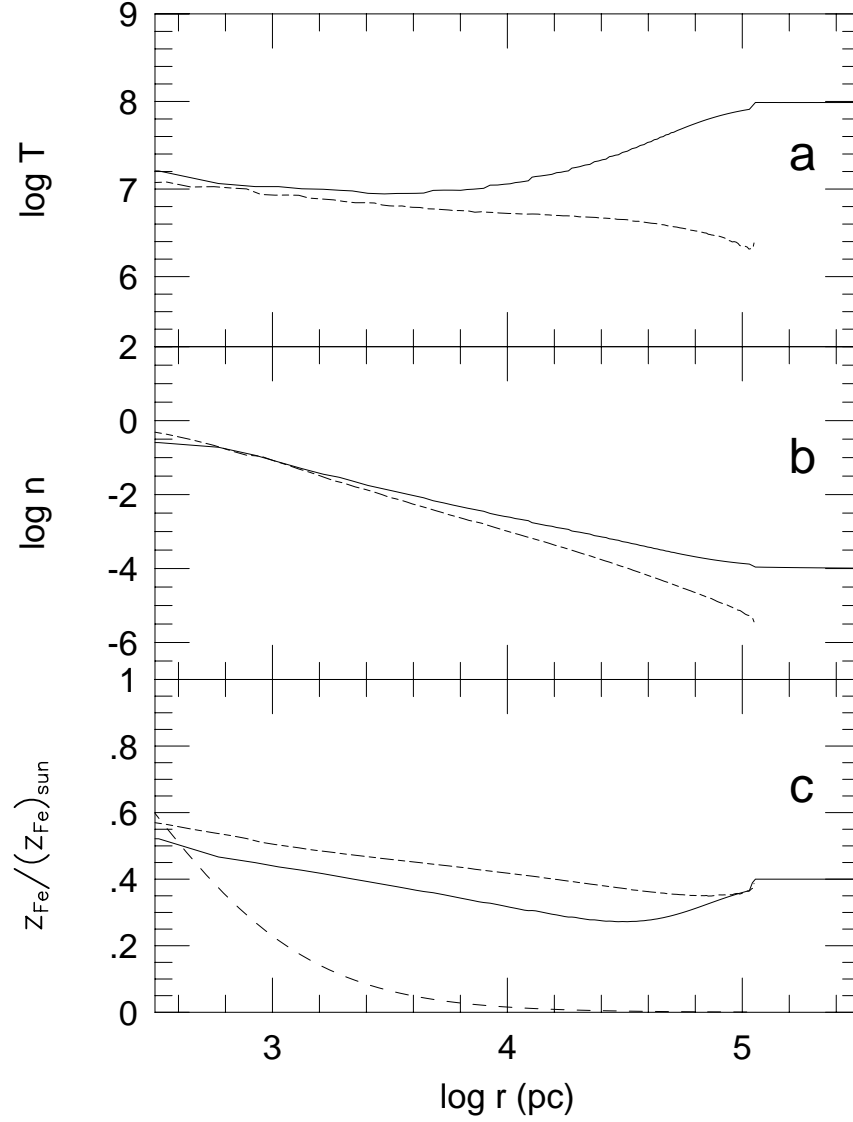


Fig. 5.— Influence of environmental cluster gas on the current properties of a galactic cooling flow. The galactic parameters are $s = 0.5$, $\text{SNU}(t_{\text{now}}) = 0.022$, and $m = 1.3$. The cluster gas has temperature $T_{cl} = 10^8$ K and density $n = 10^{-4} \text{ cm}^{-3}$ at 1 Mpc. In all plots solid lines refer to a galaxy immersed in cluster gas and the long-short dashed lines refer to the same galaxy when isolated. (a) Variation of gas temperature with radius, (b) Variation of gas density with radius, (c) Variation of the ISM iron abundance (in solar units) with radius, including that of the stars $z_*(r)$ (dashed lines).